

Interference from the Robledo DSN Transmitters to Central Madrid IMT-2000/UMTS System through Terrain Diffraction at S-Band

Christian M. Ho¹, Miles K. Sue¹, Ted K. Peng¹ and Ernest K. Smith²

¹Jet Propulsion Laboratory, California Institute of Technology, Pasadena, CA

²Department of Electrical and Computer Engineering, University of Colorado, Boulder, CO

Abstract: This study evaluates the possible interference from DSN Robledo 70-m transmitter with Madrid IMT-2000/UMTS wireless users in Spain as both systems will share the same frequency band. Using the effective earth radius, the 50 km terrain profile between Robledo and Madrid is modified and reconstructed. The diffraction propagation losses due to mountain peaks are calculated for the receivers in Madrid urban area. The mountains along the path are simplified into a rounded knife-edge and a rounded obstacle. The results show that for a near surface receiver (1.5 m above the ground) in Madrid, interference signal powers received are less than -135 dBm, which is far below the -109 dBm, the IMT-2000 wireless phone threshold. When a receiver is located at about 40 m above the ground (e.g., the top of Clock Tower of Cibeles Palace), diffraction will generate interference power less than -115 dBm. We find that our calculation results are basically consistent with those from the Longley-Rice model, while the latter has smaller loss because of the low resolution terrain profile used. As a comparison, we also find that the measurements of interference powers of -121.2 dBm at the top of Clock tower is in the range of the estimation. We conclude that the interference through the diffraction mechanism will not cause any problem to IMT-2000/UMTS users at near the surface of Madrid urban area.

1. Introduction

International Mobile Telecommunications (IMT)-2000^[1,2,3], also known as third generation wireless^[4], is moving their frequency spectrum into S-band^[5]. In Europe, this concept is also called Universal Mobile Telecommunications System (UMTS)^[6,7,8]. Progressing even further, the Spanish government has auctioned this new frequency band to the wireless industrials. The NASA Deep Space Network (DSN) has been operating powerful transmitters at S-band with an uplink frequency of 2110 – 2120 MHz and a downlink frequency of 2290 – 2300 MHz. The transmitters at three worldwide sites have both 34-m and 70-m antennas. The DSN uplink frequency (2110-2120 MHz) will overlap with the frequency band planned by the IMT-2000/UMTS terrestrial system (2110-2170 MHz). Thus, NASA Madrid DSN transmitters may interfere with UMTS forward link^[5,6] (mobile phone) users in the

neighborhood. It becomes an urgent task to examine the interference effects from, and the coordination distance of, the DSN transmitters.

Because the same frequency band is used between the DSN transmitter and IMT-2000/UMTS, the interference signals will cause a potential problem if there is not enough geographic separation. Based on ITU (International Telecommunications Union) interference propagation models^[9,10,11], there are three significant types of interference mechanisms in addition to line of sight. They are, respectively, diffraction over the spherical Earth and mountain tops, ducting and rain scattering. While diffraction and ducting propagation require the transmitted rays to have low elevation incident angles (which generally corresponds to coupling through the sidelobe of the DSN transmitting antenna), rain scattering may occur through main lobe coupling. On the other hand, ducting propagation and rain scattering create problems for very small percents of time (< 1%), while the diffraction mechanism can work almost at all time.

For transmission paths extending only slightly beyond line of sight, diffraction will be the dominant mechanism in most cases and scattering may be neglected. Conversely, for long paths (more than 100 km), the diffracted field may be hundreds of decibels weaker than the scattered or ducted field (such as, tropospheric scattering, rain scattering and ducting), and thus the diffraction mechanism can be neglected. In the previous study^[12], we have studied ducting and rain scattering interference effects at a very small percents of the time, through anomalous propagation without consideration of the terrain blockage. We also estimated diffraction losses under a very simplified assumption and without using any real terrain profiles. Through that study, we found that if there was no mountain (purely spherical earth), the coordination distance from the DSN transmitter is 70 km, beyond which the interference power is below the mobile phone threshold. If there were mountains in between, the coordination distance could be reduced to 30 km, less than the distance to central Madrid. Here, we will study the interference generated through the terrain diffraction using a detailed terrain profile around Madrid, Spain. We have basically followed the procedures described in the Recommendation (ITU-R P.452)^[9] and also referred to other ITU recommendations^[10,11] to evaluate the interference from the DSN transmitting station near Madrid, Spain.



Figure 1. DSN Robledo transmitting station and surrounding environment. The 70-m antenna is seen in the leftside of the foreground of the picture. The mountain ridges (east of the antenna) behind the antenna have higher elevation, which block the direct line of sight from the transmitter to Madrid.

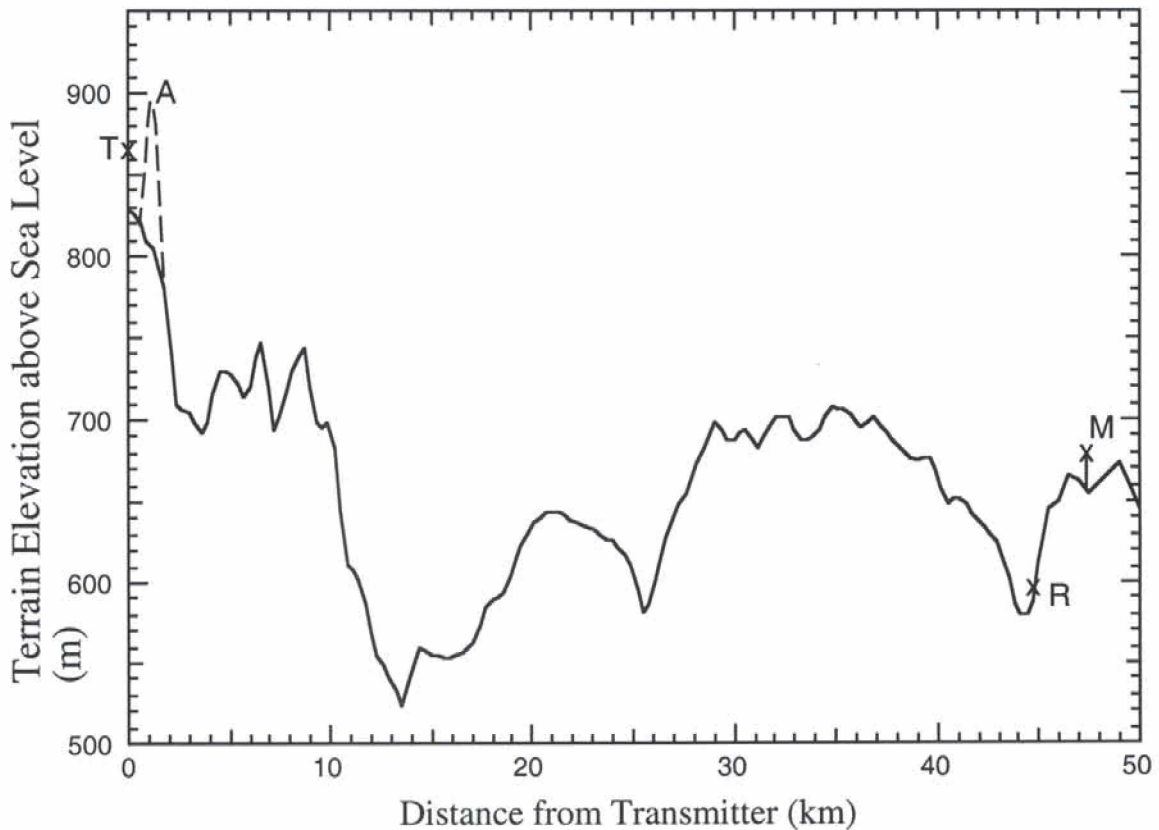


Figure 2. Low resolution terrain profiles from DSN Robledo transmitter site (T, 37 m above the ground) to Madrid, Spain. The receiver R is at central Madrid (1.5 m above the ground). M is at the top of the Clock Tower of the Cibeles Palace (east Madrid, about 40 m above the ground). A rounded peak (dash line) is added to the profile later on. Even though this peak is small, it is very important in blocking the line of sight from receivers to transmitter. The profile is plotted on a flat earth. If it is plotted on a corrected earth, the receiver M will be blocked from peak A by the nearby mountains.

2. Path Profile Analysis

NASA's DSN transmitting station in Spain is actually located at Robledo as shown in Figure 1, 44.7 km west of central Madrid. It is 47.3 km from the Robledo DSN 70m transmitter antenna to the clock tower of Cibeles Palace. We have obtained Robledo-Madrid profiles from the Institute of telecommunication Sciences (ITS) worldwide terrain database as shown in Figure 2. The terrain profile has 1.0 km resolution. The coordinates of the Robledo DSN 70 m transmitter, the central Madrid and the clock tower of Cibeles Palace are listed in Table 1. Basically this is a hilly area with a complicated terrain structure. The 70-m antenna site is actually located within a valley. Because of lower spatial resolution of the profile, some peaks which may cause important diffraction effects are not visible in the original profile. After carefully reviewing the surrounding environment around the DSN site, we find that a nearby mountain ridge which rises above eastward of the 70-m antenna just blocks the line of sight from the transmitter to receivers, in central Madrid. The high resolution maps show that this ridge consists of two small peaks which are 1.2 to 1.5 km from the transmitter respectively. Peaks have a 1.5° elevation angles relative to the 70 meter antenna. The antenna's elevation is defined as the height of the center axis of its dish above the sea level. Thus, eastside mountain peaks will cause significant diffraction attenuation to interference signals. Around the Robledo DSN site, we have used the high resolution map to modify the original profile along the great circle by adding the peak with certain thickness (dash line in Figure 2). Even though the site of the transmitter is at a higher elevation than Madrid, there are several mountain peaks between. The central Madrid is also in a valley, with a rounded mountain peak on its westside. Thus there is no common horizon for the transmitter and the receivers. This is a multiple-obstacle diffraction interference problem.

Table 1. Coordinates of Three Locations

Locations	Latitude	Longitude	Elevation, m
Robledo Transmitter, T	40°25'52"N	4°14'53"W	865
Central Madrid, R	40°25'1"N	3°43'31"W	587
Cibeles Palace, M	40°25'06"N	3°41'18"W	680

2.1. Median Effective Earth's Radius: Because the near Earth space is filled with atmospheric gases which decrease in density with altitude, the radio wave ray will be bent as it passes through the medium. The ray can even reach some objects beyond the line of sight. The severity of the bending is determined by the gradient of the refractive index near the earth's surface. In order to represent the radio ray as a straight line, at least within the first few kilometers above the surface, an "Effective Earth's Radius" is defined as a function of the refractivity gradient, ΔN . The median effective Earth radius factor k_{50} ($p = 50\%$) for the path is determined as

$$k_{50} = \frac{157}{157 - \Delta N_{50}} \quad (1)$$

The median value of effective earth radius, a_e , is a product of true earth radius (6371 km at midlatitude) with k_{50} :

$$a_e(50\%) = 6371 \cdot k_{50} \quad (\text{km}) \quad (2)$$

From the world map of average annual ΔN values, Around Madrid-Robledo area, $\Delta N_{50} = 45$ N-units/km. Thus $k_{50} = 1.402$, the median effective earth radius is 8931 km.

2.2. Construction of path profile: Using the effective Earth radius, we can modify the elevation of terrain profile using the following equation.

$$y_i = h_i - x_i^2 / 2a_e \quad (3)$$

The modified terrain profile is shown in Figure 3 using the median effective Earth radius. As constructed, in this plot, all radio wave rays become straight lines. The bending effects due to atmospheric diffraction have been removed by making the earth surface flatter. All distances and heights will be derived from this modified plot. To construct this plot, elevations h_i of the terrain are read from topographic maps versus their distance x_i from the transmitting antenna. The terrain profile is plotted by modifying the terrain elevations to include the effect of the average curvature of the radio ray path and of the earth's surface. The solid curve near the bottom of the figure indicates the shape of a surface of constant elevation ($h = 0$). Clearly, this is a path with two radio horizons for transmitter T and receiver R. The vertical scales of the figure are exaggerated in order to provide a sufficiently detailed representation of terrain irregularities. Plotting terrain elevations vertically instead of radially from the earth's center

leads to negligible errors where vertical changes are small relative to distances along the profile.

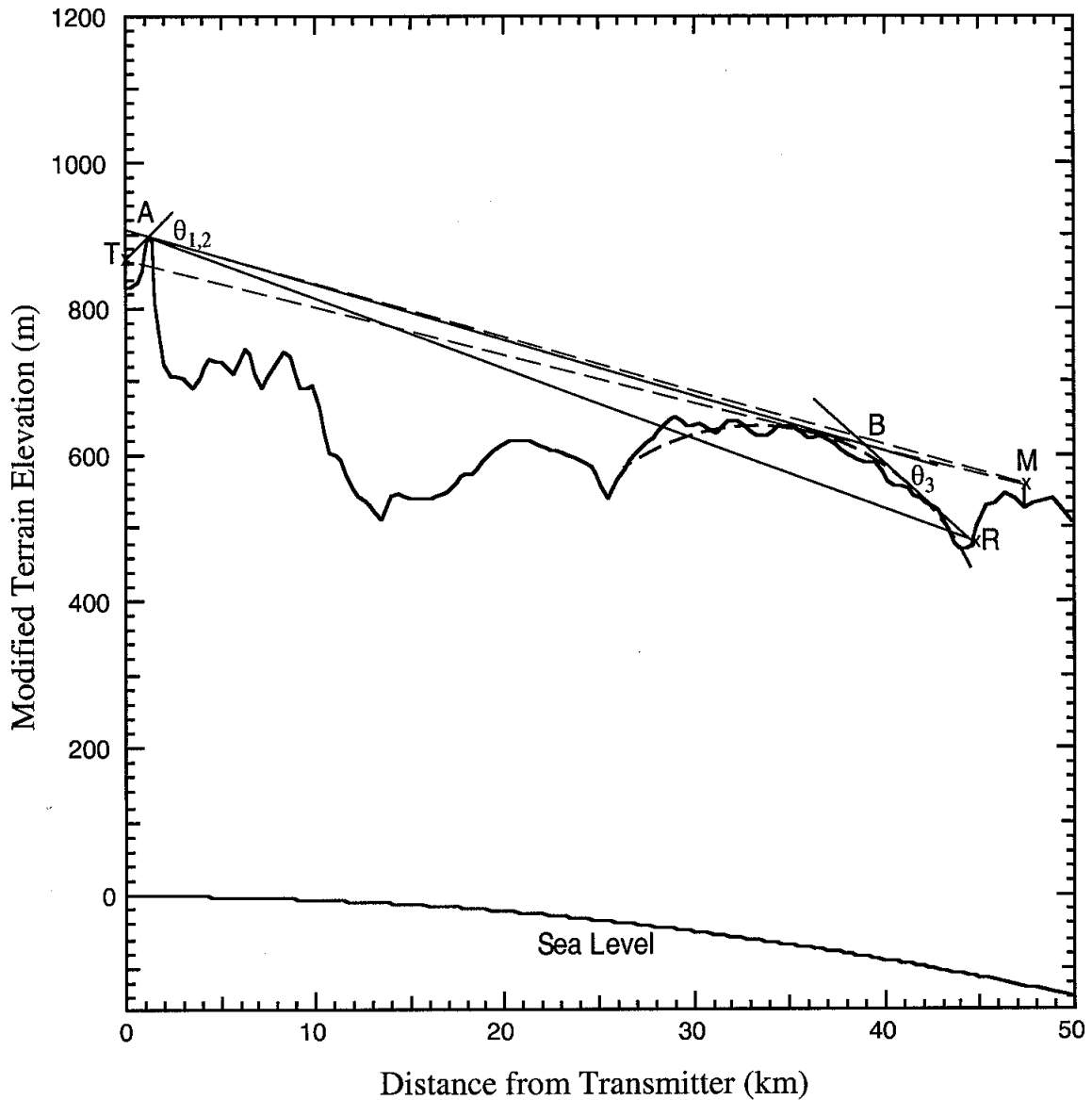


Figure 3. The modified topographic terrain profile from Robledo to Madrid, Spain. A small peak (A) with rounded top has been added to the profile. Receiver R at central Madrid (1.5 m above the ground) is within the shadow of the mountain. The receiver M at the top of the Clock Tower of Cibeles Palace (east of central Madrid, about 40 m above the ground) has direct view to the top of peak A. This modification is equivalent to plot the terrain profile with a curved earth with a radius of $a_e = 1.402$ earth radius.

2.3. Diffraction for Double Isolated Peaks. There is only one mountain peak which blocks receiver M from transmitter T, while two isolated obstacles block the direct line of sight from receiver R. Based on the method of dealing with double isolated knife-edges recommended

in ITU-R P.526^[13], we can apply diffraction theory to each obstacle separately. a) The first diffraction path, defined by the distances a and b (transmitter, T – first ridge, A – second ridge, B), gives a loss L_1 ; b) The second diffraction path, defined by the distance b and c (first ridge, A – second ridge, B – receiver, R), gives a loss L_2 . The two losses are then added together to obtain the diffraction attenuation over the entire path. A correction term L_c may be added to take into account the separation b between the edges. This method is illustrated in Figure 4.

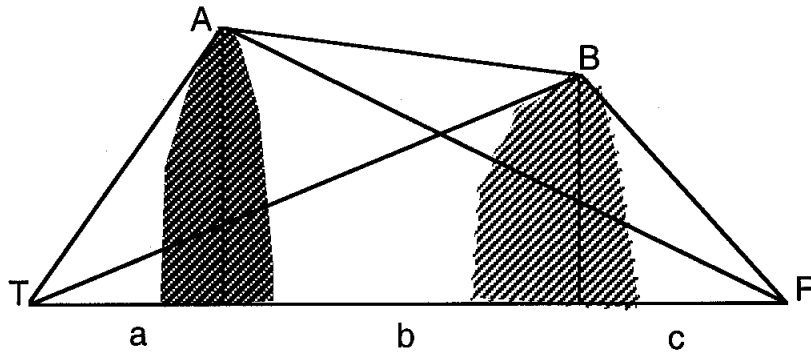


Figure 4. A procedure to calculate double isolated edge diffraction losses for receiver R.

3. Diffraction Losses over the Path

3.1. Peak A (A Rounded Knife-Edge) Relative to Points B and M. At first, we calculate the diffraction loss over peak A. These small twin peaks have been approximated by a rounded knife edge with a thickness of 300 m. As we will show later, the mountain thickness will cause a significant loss in addition to a pure knife-edge loss. The angular distance, θ , is the angle in radians between horizon rays from transmitter T and from receiver B or M in the great circle plane and is also the minimum diffraction angle.

$$\theta = d/a_e + \theta_{et} + \theta_{er} \quad (4)$$

where d is the distance between the transmitter and receiver at sea level, the a_e is the median effective earth radius. The horizon ray elevation angles θ_{et} relative to transmitter and θ_{er} relative to receiver may be computed using the following equations:

$$\theta_{et} = \frac{h_{Lt} - h_{ts}}{d_{Lt}} - \frac{d_{Lt}}{2a_e} \quad (5)$$

and

$$\theta_{er} = \frac{h_{Lr} - h_{rs}}{d_{Lr}} - \frac{d_{Lr}}{2a_e} \quad (6)$$

where h_{Lr} , h_{Lr} are the elevations of horizon obstacles and h_{ts} , h_{rs} are elevations of transmitting and receiving antennas, all above mean sea level (AMSL), respectively. The transmitter antenna is 37 m above the ground, while the receiver in Madrid downtown (R) is 1.5 m above the ground and the receiver at the top of clock tower of Cibeles Palace (M) is about 40 m above the ground. The d_{Lt} and d_{Lr} are sea level arc distances from each antenna to their radio horizon obstacles respectively. As a general rule, the location (h_{Lr} , d_{Lr}) or (h_{Lr} , d_{Lr}) of a horizon obstacle is determined from the terrain profile by the above equation to test all possible horizon locations. The correct horizon point is the one for which the horizon elevation angles θ_{et} and θ_{er} are a maximum. When the trial values are negative, the maximum is the value nearest zero. The horizon elevation angle is defined here as the angle viewed from the center of the earth-station antenna, between the horizontal plane and a ray that grazes the visible physical horizon in the direction concerned; d_1 and d_2 are the distances from the transmitter and receiver respectively to the top of the peak. For practice, d_1 and d_2 may be replaced by d_{Lt} and d_{Lr} , because the peak height is relatively small compared to the horizontal distance. D_s is thickness of the rounded top and h_r is its height relative to the baseline TB or TM. All parameters for this study are listed in Table 2 for peak A and are also shown in Figure 5.

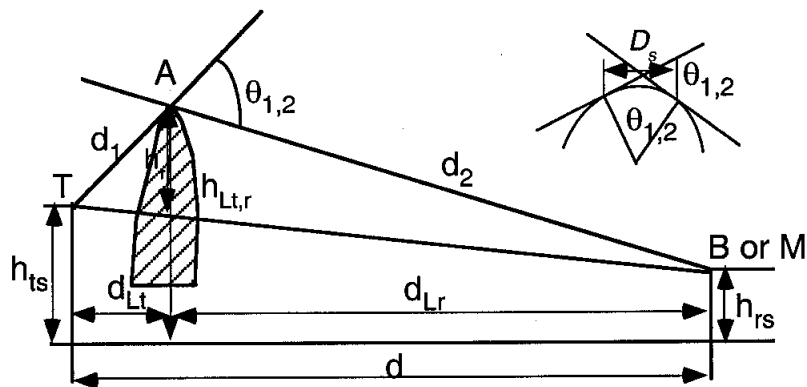


Figure 5. Geometric parameters for a rounded knife edge diffraction losses relative to point B and receiver M. Note that vertical scales of the figure have been much enlarged relative to the horizontal scales. The inserted shows how the radius of the rounded mountain top is defined using a similar scale.

Table 2. Parameters for Peak A (A Rounded Knife Edge)

Paths	d , km	d_1 , km	d_2 , km	d_{L1} , km	d_{L2} , km	h_{ts} , km	h_{rs} , km	h_{L1} , km	h_{L2} , km	h_r , km	D_s , km
TAB(1)	38.8	1.2	37.6	1.2	37.6	0.865	0.700	0.896	0.896	0.031	0.30
TAM(2)	47.3	1.2	46.1	1.2	46.1	0.865	0.680	0.896	0.896	0.031	0.30

For a rounded knife edge, the diffraction loss includes two parts

$$A = J(v) + T(m, n) \quad (7)$$

where $J(v)$ is a loss due to an equivalent knife-edge placed with its peak at the vertex point, $T(m, n)$ is the additional loss due to the curvature of the obstacle.

To calculate $J(v)$, we need to first find the parameter, v , which is defined as

$$v = \theta \sqrt{\frac{2d_1d_2}{\lambda d}} \quad (8)$$

where wavelength $\lambda = 1.42 \times 10^{-4}$ km for the radio wave at S band (2115 MHz). The diffraction loss for a single knife edge is

$$J(v) = 6.9 + 20 \log(\sqrt{(v - 0.1)^2 + 1} + v - 0.1) \quad \text{dB} \quad (9)$$

Then we need to calculate the radius r of the rounded knife-edge. A simple way to find r is

$$r = \frac{D_s}{\theta} \quad (10)$$

where D_s is the distance (or thickness) of the rounded mountain top.

The curvature loss

$$T(m, n) = k(n) \cdot m^{b(n)} \quad (11)$$

where parameter

$$m = r \left[\frac{d_1 + d_2}{d_1 d_2} \right] / \left(\frac{\pi r}{\lambda} \right)^{1/3} \quad (12)$$

$$n = h_r \left[\frac{\pi r}{\lambda} \right]^{2/3} / r \quad (13)$$

$$b = 0.73 + 0.27[1 - \exp(-1.43n)] \quad (14)$$

and

$$k = 8.2 + 12.0n \quad (15)$$

Using the median effective Earth radius, equations (4) - (15) and parameters listed in Table 2, we obtain $\theta_1 = 0.0333$ radians, $v_1 = 4.257$, $J_1(v) = 25.42$ dB, $T_1 = 19.20$ dB, and $A_1 = 44.62$ dB respective to point B; $\theta_2 = 0.0331$ radians, $v_2 = 4.250$, $J_2(v) = 25.40$ dB, $T_2 = 19.66$ dB, and $A_2 = 45.06$ dB respective to receiver M. Both losses have similar values. These results are list in Table 3. Here we have used subscribe numbers 1 relative to point B, 2 to M and 3 to R, respectively.

Table 3. Resultant Parameters and Diffraction Losses for Three Paths

Paths	θ , rad	v	$J(v)$,dB	r , km	m	n	b	k	T , dB	A , dB
TAB (1)	0.0333	4.257	25.42	9.0	0.129	11.75	1.0	149.4	19.20	44.62
TAM (2)	0.0331	4.250	25.40	9.0	0.132	11.75	1.0	149.2	19.66	45.06
ABR (3)	0.0164	4.40	25.70	301.8	0.310	8.24	1.0	107.1	32.12	57.82

3.2. Peak B (Isolated Rounded Obstacle) Relative to point R. Because the isolated rounded obstacle (Peak B) does not block the receiver M from viewing the Peak A, the diffraction loss of Peak B to the receiver M is zero. We only need to calculate the diffraction loss to receiver R. The mountain ridge B may be approximated as a rounded obstacle. The geometry for an idealize rounded obstacle is shown in Figure 6. Here, the rounded obstacle is considered to be isolated from the surrounding terrain. We have used a 2-D cylinder with a radius r to fit the rounded obstacle.

Two straight lines tangential to the cylinder from points A and R cross each other at point B as shown. h_r is the obstacle's height from point B to the baseline AR, D_s is the horizontal distance between two tangential points on the cylinder, d_{sl} is the horizontal distance between the point B to the left-side tangential point, while d_{sr} is the horizontal distance to the right-side tangential point. These parameters will be used to calculate the radius r . All parameters for the diffraction loss calculation for Peak B is listed in Table 4.

For the rounded obstacle, the radius is obtained using

$$r = \frac{2D_s d_{st} d_{sr}}{\theta_2 (d_{st}^2 + d_{sr}^2)} \quad (16)$$

where

$$D_s = d - d_{Lt} - d_{Lr} \quad (17)$$

Using the median effective Earth radius, equations (16), and (17), some equations listed in the previous subsection, and parameters in Table 4, we obtain $\theta_3 = 0.0164$ radians, $v_3 = 4.40$; and $J_3(v) = 25.70$ dB for equivalent knife-edge loss; $D_s = 5.2$ km, $r_3 = 301.8$ km, and $m = 0.31$, $n = 8.24$; $b = 1.0$; $k = 107.06$, $T_3 = 32.12$ dB for curvature loss. Finally, the loss for the rounded obstacle is $A_3 = 57.82$ dB.

Table 4. Parameters for Peak B (An Isolated Rounded Obstacle) for Path ABR (3)

d , km	d_1 , km	d_2 , km	d_{Lt} , km	d_{Lr} , km	h_{ts} , km	h_{rs} , km	h_{Lt} , km	h_{Lr} , km	d_{st} , km	d_{sr} , km	h_r , km
43.5	37.6	5.9	37.6	5.9	0.896	0.587	0.700	0.700	2.2	3.0	0.07

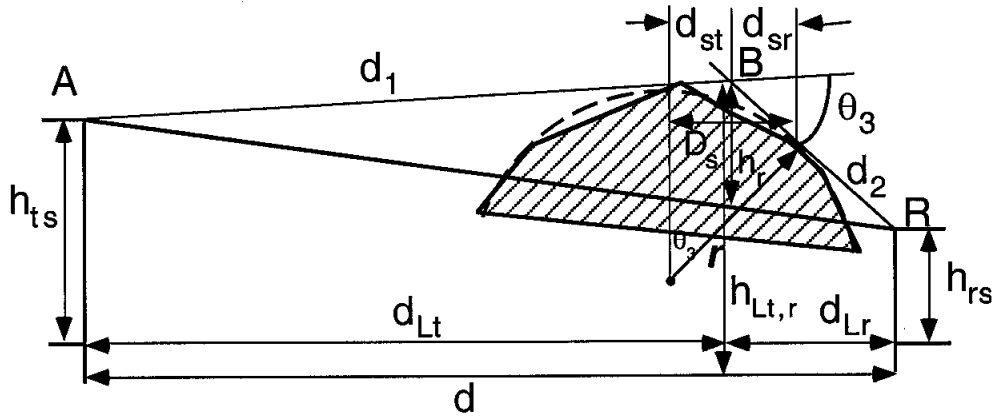


Figure 6. Geometry of diffraction parameters for a rounded obstacle R. The figure also shows how the radius of the obstacle is defined when D_s is much larger than h_r .

3.3. Total Diffraction Losses. Diffraction loss relative to receiver R is two peak loss combination as shown in Figure 4^[13]

$$L_d = A_1 + A_3 + L_c \quad (18)$$

where L_c is a correction term ($= 0.02$ dB). Thus $L_d = 102.46$ dB for receiver R. For other two locations (B and M), because only one peak loss is involved, L_d is same as the values of A listed in Table 3. For receiver M, L_d is 45.06 dB.

The actual diffraction loss is always greater than the theoretical loss calculated here, because of other possible terrain effects, such as surface roughness, clutter, etc. These factors can cause some additional loss ranging usually about 10 dB.

Total propagation losses through the terrain diffraction are

$$L = L_b + L_d \quad (19)$$

where L_b is free space basic transmission loss

$$L_b = 32.45 + 20 \log f + 20 \log d \quad (20)$$

for signal frequency f in MHz, distance d in km. Thus for receiver R, we have $L_b = 131.96$ dB and $L = 234.40$ dB.

For receiver M, the diffraction loss over peak A is 45.06 dB. Thus when $L_b = 132.46$ dB, we have $L = 177.52$ dB. Both receivers at points R and M, only 2.6 km apart, have a 56.88 dB difference in diffraction loss. This indicates that diffraction loss is very sensitive to the topographic location of the receiver relative to the shielding mountains. Here we have neglected the gaseous absorption loss in the surface^[14], because this loss is very small at S-band.

3.4. Percent Time Dependence: Diffraction loss can also have time dependence, because the gradient of atmospheric refractivity is a function of time. This will affect the effective earth's radius, a_e . When the refractivity index gradient becomes very large at very small percent of time, the anomalous effective earth radius applies. Anomalous time percentage $\beta_0(\%)$ is defined as the percent of the time when the refractive index gradient exceeds 100 N-units/km in the first 100 m of the lower atmosphere at the central latitude, φ , under consideration.

$$\beta_0 = 10^{-0.015|\varphi|+1.67} \mu_1 \mu_2 \quad (\%) \quad (21)$$

where μ_1 and μ_2 are parameters depending on the degree to which the path is over land and water. For Madrid-Robledo path, when $\varphi = 40^\circ$, we have $\mu_1 = 0.144$, $\mu_2 = 1.566$ and $\beta_0 = 2.64\%$. Because $k(\beta_0)$ is defined as $3.0^{|\beta_0|}$, thus the anomalous effective earth radius $a_e(\beta_0) = 6371 \cdot k(\beta_0) = 19113$ km.

For $p = 50\%$, $L_d(50\%)$ is computed using the median effective earth radius $a_e(50\%)$. We have the median diffraction loss $L_d(50\%) = 102.46$ dB for receiver R.

For $p \leq \beta_0\%$, $L_d(\beta_0)$ is computed using the anomalous effective earth radius, $a_e(\beta_0)$, for an anomalous time percentage $\beta_0(\%)$. Following the same procedure as shown in previous section, we have anomalous diffraction loss $L_d(\beta_0) = 99.54$ dB, only 2.92 dB less than the median loss.

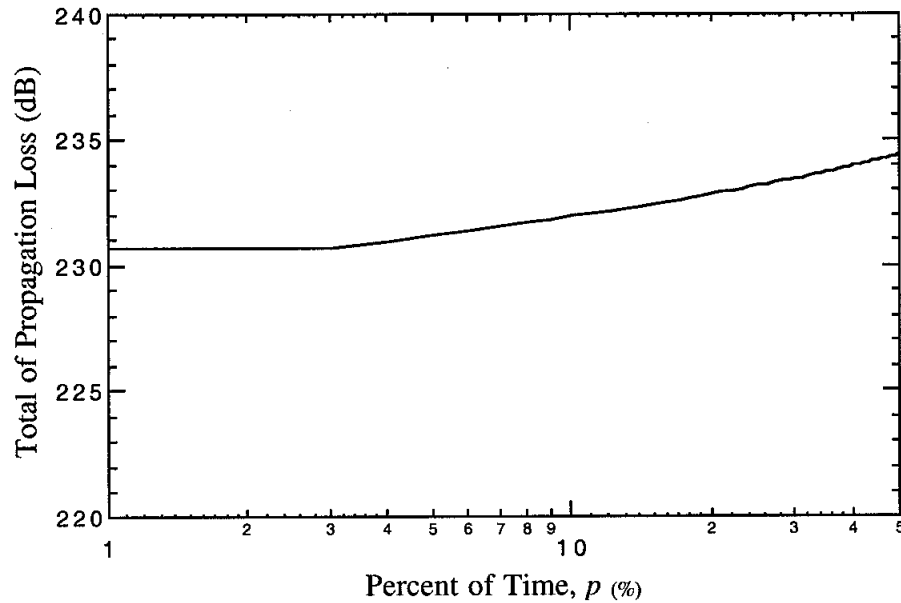


Figure 7. Total propagation loss over two mountain peaks for receiver R as a function of percent of time.

For $\beta_0\% < p < 50\%$, $L_d(p)$ is given by^[9]:

$$L_d(p) = L_d(50\%) - F_i(p)[L_d(50\%) - L_d(\beta_0)] \quad (22)$$

where $F_i(p)$ is an interpolation factor based on a log-normal distribution of diffraction loss over the range $\beta_0\% < p < 50\%$ given by

$$F_i(p) = I(p/100) / I(\beta_0/100) \quad (23)$$

where $I(p/100)$ is the inverse cumulative normal function.

Finally, the total propagation loss as a function of percent time, p , is

$$L(p) = L_b + L_d(p) \quad (24)$$

where we have neglected a small correction term $E_{sd}(p)$. The result for receiver R is shown in Figure 7.

3.5. Interference Signal Powers. Using the fundamental relation:

$$P_r = P_t + G_t - L(p) + G_r \quad (\text{dB}) \quad (25)$$

we can estimate the interference power (P_r) received by an IMT-2000 personal station. Here, P_t is the transmission power, and G_t is the transmitter's antenna gain toward the physical horizon at the horizon elevation angle under consideration^[15].

Under the normal situation, for Robledo 70-m antenna facility, $P_t = 20 \text{ kW} = 43 \text{ dBW}$ (73 dBm). Its backlobe antenna gain ($G_t = -10 \text{ dB}$)^[16] points to Madrid direction. Antenna gain (G_r) of personal station receiver (mobile phone) is 0 dB at Madrid 1.5 m above the ground and the interference threshold is $-139 \text{ dBW} = -109 \text{ dBm}$ ^[11]. Thus, we have $P_r = 63 \text{ dBm} - L(p)$. At central Madrid for receiver R, because the median propagation loss $L(50\%) = 234.4 \text{ dB}$, the median interference power received $P_r = -171.4 \text{ dBm}$. This is far less than the IMT-2000 system threshold. For receiver M, $P_r = -114.52 \text{ dBm}$, also below the threshold.

For a very limited time, the 70-m transmitter transmits with a maximum power $P_t = 200 \text{ kW} = 53 \text{ dBW}$ (83 dBm). For the worst scenario, due to mechanical limitations, the antenna has a 10° minimum elevation angle with pointing Madrid's azimuth. The eastside mountain peak relative to the antenna has a 1.5° elevation angle. Thus, the mountain top has an angle of 8.5° off from the antenna's boresight. Based on the ITU model^[16], the antenna gain with a 8.5° off angle from the antenna's boresight gain (62 dBi) is 5.7 dBi for a far field scenario. Thus, we have $P_r = 88.7 \text{ dBm} - L(p)$ for the far field calculation. However, this is a near-field problem because the nearby mountain peak is only 1.2 km away from the transmitter. The distance is much less than the first Fresnel distance $(D^2/2\lambda = 17 \text{ km})$ ^[17], where D is the diameter of the antenna dish (70 m) as shown in Figure 8. The beam radiated from the antenna aperture is so

narrow (the beam width is less than the dish's diameter or parallel beam) that the antenna gain at a distance l ($180 \text{ m} = 2.6 D$) from the beam center axis is about $-3 \text{ dBi}^{[18]}$, 8.7 dBi less than the far field antenna gain. Thus, for this worst case, the interference power should be $P_r = 80 \text{ dBm} - L(p)$. At the central Madrid location for receiver R, interference power received is $P_r = -154.4 \text{ dBm}$. This is still far less than the IMT-2000 system threshold. For receiver M, the interference power received $P_r = -97.52 \text{ dBm}$. This is 11.48 dB over the threshold. However this situation will happen very rarely.

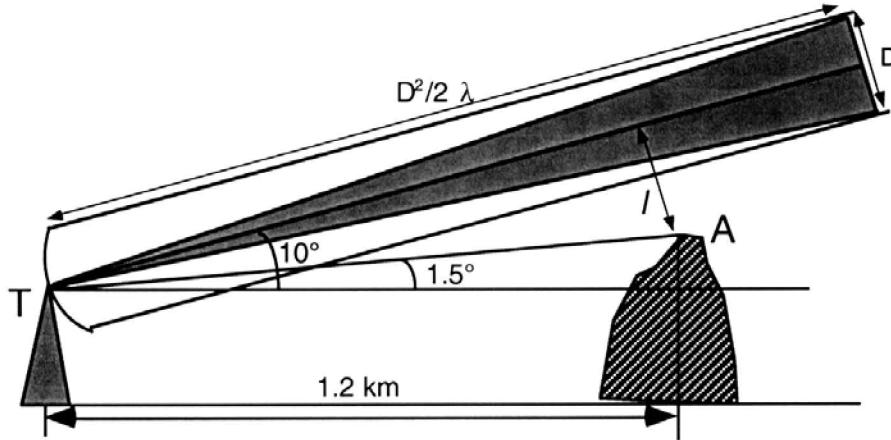


Figure 8. A sketch shows the DSN antenna has a 10° elevation angle toward Madrid. The nearest mountain top has a 1.5° elevation angle and a distance of 1.2 km which is far less than the first Fresnel distance. Thus, the point A is outside of the beam radiated from the antenna aperture and there is much low radiation power at the near field.

4. Comparison with Longley-Rice Model

The Longley-Rice model^[19,20] is an engineering model. The model is widely accepted and used by telecommunication industry and government agencies for interference evaluation. The model was developed by ITS in 1960s–70s after extensive review of theoretical studies in interference propagation, and has also been compared with an extensive base of measurements with good prediction credibility.

Using a low resolution terrain profile as shown in Figure 2, the 3-D interference signal field strength contour is calculated by ITS with the Longley-Rice terrain diffraction model, as shown in Figure 9. Because the terrain profile does not include peak A and other small peaks, we expect that there are smaller losses than we obtained previously. Figure 9 shows

interference signal power (dBm) received by UMTS users with a 200 km x 200 km extent, centered at DSN Robledo transmitter site.

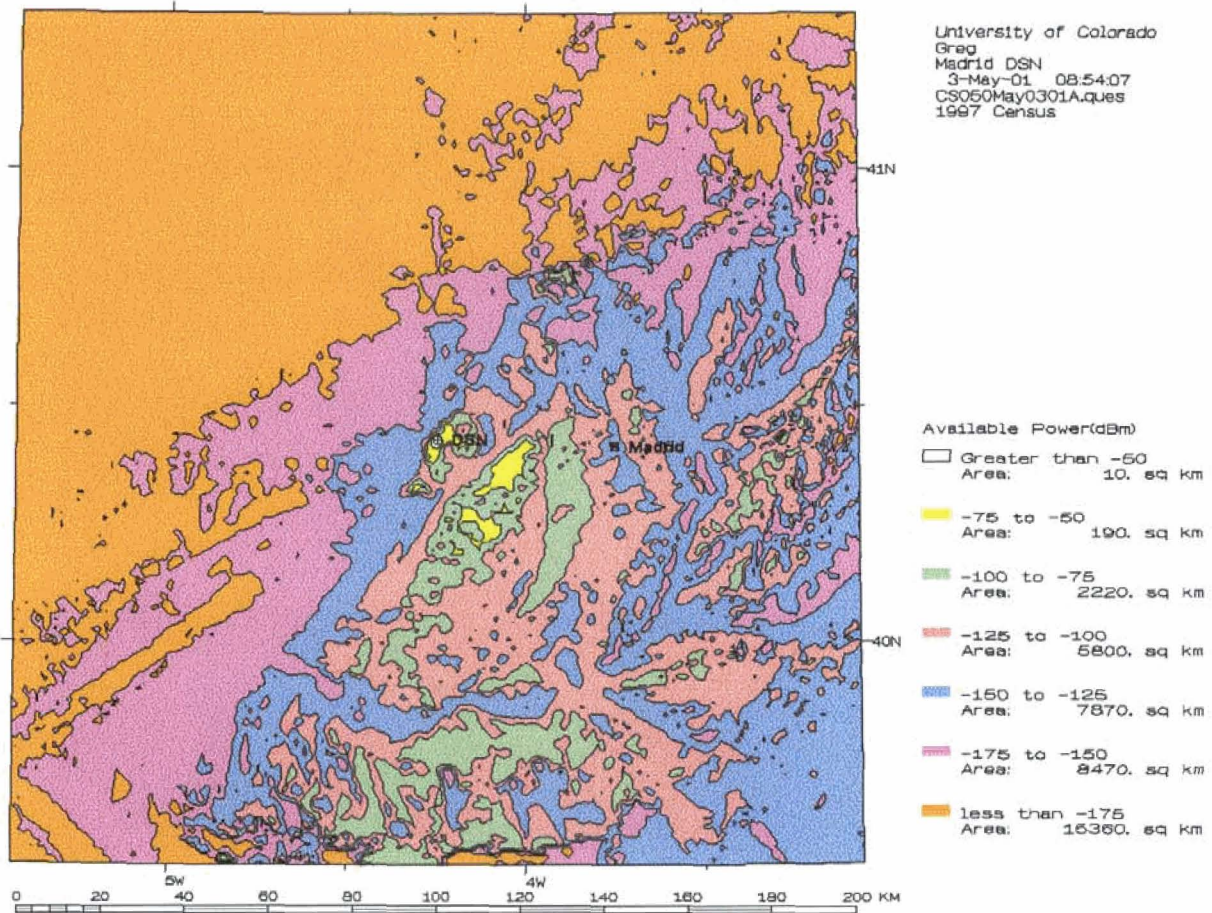


Figure 9. A contour map showing interference signal powers received by UMTS users in the areas surrounding the DSN Robledo 70 m transmitter. The contours have 7 color levels from -50 dBm to -175 dBm and each with 25 dBm range.

To make this contour map, the following parameters have been used. Transmitter power: $P_t = 20$ kW; transmitter antenna elevation: $h_{ts} = 865$ m, (37 m above the ground); transmitter antenna gain: $G_t = -10$ dB; receiver antenna gain: $G_r = 0$ dB; receiver antenna elevation: 1.5 m above the ground everywhere. From Figure 9 we can see that following the terrain elevation changes, interference power also changes. In the valleys and the mountain sides shadowed from the transmitter, the interference power decreases and the diffraction loss increases sharply. At the mountain tops and the sides toward the transmitter, the interference power increases and the diffraction loss decreases. In the deep shadow regions (with large

receiver elevation angles), there are large diffraction losses. Interference signals are significantly shielded by the mountains. Away from the shadows, the diffraction loss becomes small and interference signals become stronger.

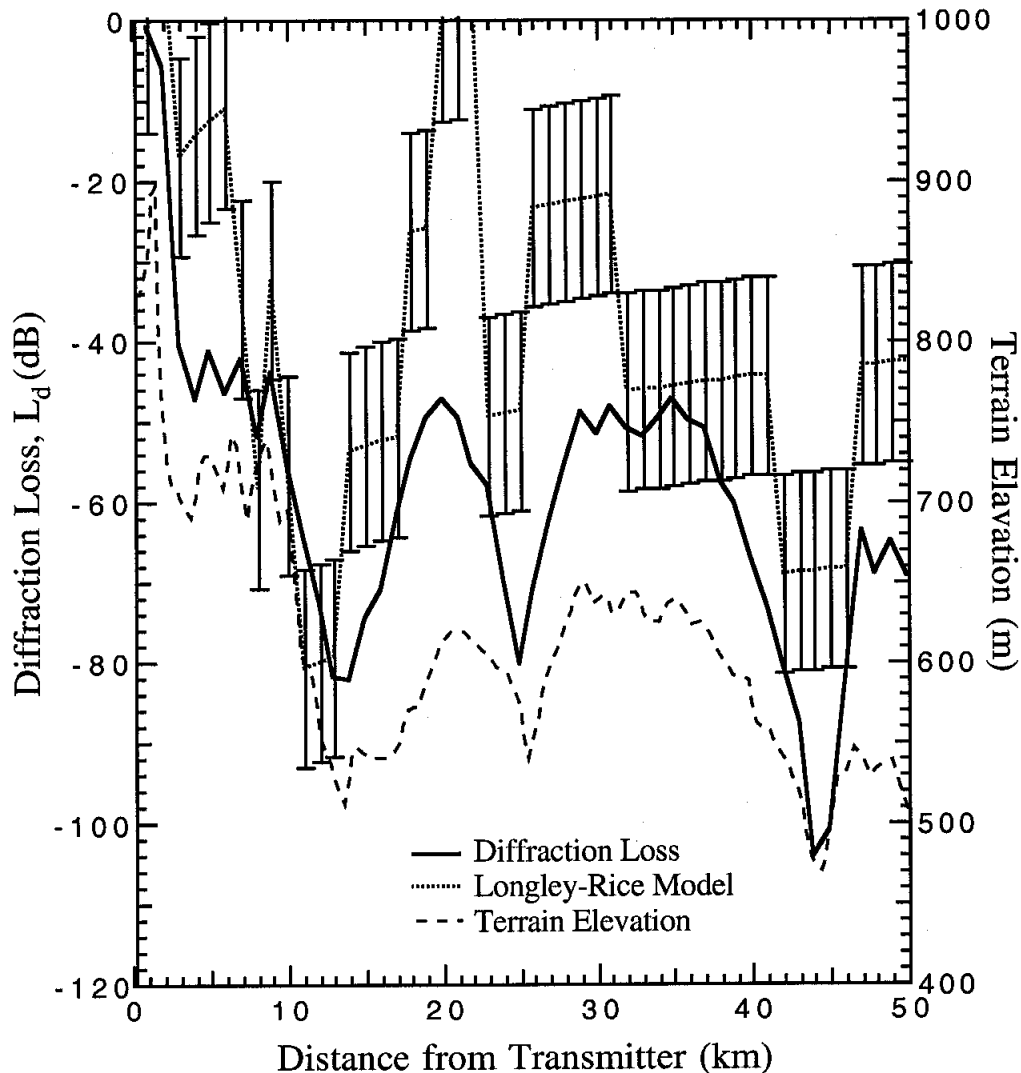


Figure 10. Diffraction losses as function of distance from Robledo DSN transmitter from this study (solid line). The losses from Longley-Rice model (dotted line) are also shown with error bars. As a comparison, the terrain elevation profile is shown using the right axis.

Along the Robledo–Madrid line we can make a cut of the contour map to obtain the interference power as a function of the distance from the Robledo transmitter. To make the comparison, the diffraction loss profile instead of interference power is shown in Figure 10. The terrain diffraction loss from this study is shown by a solid line. To obtain this continued profile with distance, we have followed the procedure described in Section 3 to calculate the

losses at all key points. For Longley-Rice model results, the diffraction loss (L_d) due to the terrain excludes the free space loss using equation $-L_d = P_r - 63 \text{ dBm} + L_b$, where P_r is middle values read from Figure 9 for each color level with a $\pm 12.5 \text{ dB}$ error bar, and L_b is calculated from equation (20). As a reference, the terrain elevation profile along the cut is also shown. Both diffraction losses from our calculation and from the Longley-Rice model (dotted line) have similar trends. Both diffraction loss profiles correlate well with terrain elevation profiles. That is, at valleys there are large losses, while at mountain ridges, small losses. However, there are much larger losses from our calculation than those from Longley-Rice model, because we have included an extra loss due to Peak A (a rounded knife-edge). In a separate study using high resolution (90 m) terrain profile, Longley-Rice model generates much larger diffraction losses (by 20 – 30 dB) than low resolution results shown in Figure 9. This result (restricted data, results cannot be published) is consistent with our calculation (solid line in Figure 10). Because the result from higher resolution data is always closer to actual losses, we believe that our result will more closely approach real measurement results as will be shown in next section.

5. Comparison with Experiments

The Spanish government^[21] has performed experimental measurements on DSN interference signal powers. They made several measurements around the Robledo 70 m transmitter site using a spectrometer. Because the diffraction loss variations are sensitive to location and elevation angle relative to the mountain peaks, the comparison between the measurements and model calculations needs to be made by using exactly the same locations. Madrid is a large city with a range of elevations. One measurement (Point M) in Madrid was made on November 18, 1999 at the top of the clock tower of Cibeles Palace. The elevation of the tower is 680 m, about 40 m above the ground. At 2115 MHz, the measured interference signal level was -87 dBm with an 8-dBi spectrometer antenna. During this time, the DSN Robledo 70-m antenna was transmitting 225 kW signals with a 10° elevation angle. For a mobile phone using an omni antenna with 0 dBi gain, this received interference level would be $(-87 \text{ dBm} - 8 \text{ dBi}) -95 \text{ dBm}$. Most of the time DSN transmits 20 kW signals with a -10 dBi antenna gain. Normalizing to this transmitting level, the same mobile phone would

receive -121.2 dBm interference signals. This is 12.2 dB higher than the mobile phone's threshold. Our calculation shows a -115 dBm interference power received at this location (40 m above the ground). This is 6.2 dB higher than the measurement.

Another measurement (Point H) was taken at a location: $40^{\circ}25'35''\text{N}$, $4^{\circ}0'10''\text{W}$, 670 m. This location is not along the Robledo-Madrid line. It is at a distance of 22.8 km from Robledo and 6.3 km south of the line of Robledo-Madrid. Normalizing the -72.5 dBm measurement (for 20 kW, and -8 dB antenna gain) yields -106.7 dBm. We have shown both measurements M and H in Figure 11 using special markers.

The interference powers received for a normal case, based on terrain profile calculations are also shown in Figure 11. They include signal powers through terrain diffraction near the ground and 40 m above the ground respectively, from the Longley-Rice model near the ground, and from line-of-sight (LOS) free space propagation. Here we assume "near the ground" is on the street level and without any building shielding. Actually the building shielding can easily cause more than 10 dB additional loss. Thus any measurement on the street level inside the city should show less interference powers than we showed here. We can see that the measurement values are close to the curve for a receiver 40 m above the ground. Point H measurement result is slightly above the 40 m interference curve. This is probably due to a different terrain profile from what we used. Thus, our prediction from terrain diffraction is basically confirmed by the measurements. Using these calculations, we can also predict interference levels at other locations and with different heights above the ground. For the worst case performance, we only need to shift two curves up by 17 dB for both near the ground and 40 m above ground. We see that interference powers near the ground at most Madrid areas are still below the threshold.

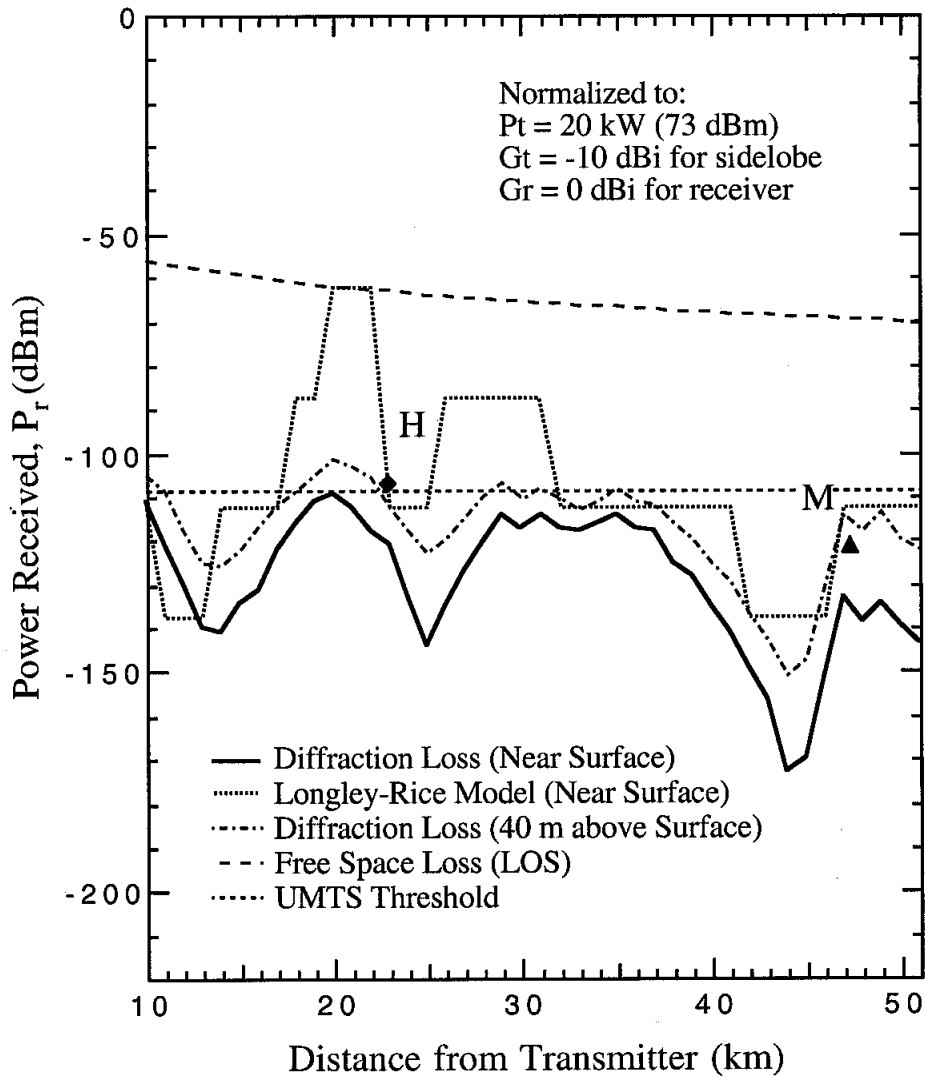


Figure 11. The interference signal power received from calculations through the terrain diffraction loss (1.5 m and 40 m above the ground), from Longley-Rice model, and from line of sight (LOS) propagation through free space. Two experimental measurements at locations M and H are also shown using markers. The UMTS mobile phone threshold (-109 dBm) is also shown.

6. Summary

In Europe, IMT-2000/UMTS users will soon start to use the new frequency band which overlaps NASA DSN uplink frequency at S-band. This study has investigated to what degree the possible interference from DSN Robledo 70-m transmitter will affect 3rd generation wireless users in the Madrid urban area. Using effective earth radius, the 50 km terrain profile between Robledo and Madrid is modified and reconstructed. The diffraction

propagation losses by mountain peaks are calculated relative to the receivers in the Madrid urban area. The mountains along the path are simplified into a rounded knife-edge and a rounded obstacle. Two types of cases are studied corresponding to different transmitting powers and antenna gains. Under normal situation, the DSN station transmits 20 kW power and with a back lobe antenna gain (-10 dBi), while under worst scenario (< 1% of time) transmitting powers can reach as much as 200 kW and antenna has a 10° elevation angle pointing to Madrid. The results show that diffraction losses significantly depend on receiver's topographic locations and elevation angles relative to shielding mountains. For a near surface receiver (1.5 m above the ground) in Madrid, interference signal powers received are less than -135 dBm, which is far below the -109 dBm, the IMT-2000 wireless phone threshold. When a receiver is located at 40 m above the ground, diffraction will generate an interference power of about -115 dBm. We have also compared our calculations with those from the Longley-Rice model using a low resolution terrain profile. Both results are basically consistent, even though the latter has higher interference powers because fewer mountain peaks are included. In comparison with measurements, we find that interference levels of -121.2 dBm at the top of the Clock tower of Cibeles Palace, about 40 m above the ground, is in the range of the estimation, considering errors between modeling calculations and actual losses. At some high buildings within Madrid city, which are less shaded from the mountain peaks, the interference powers may exceed the wireless phone threshold only under worst conditions. However, in the almost all areas of Madrid at the surface levels, interference through the diffraction will not cause any problem to IMT-2000/UMTS users under both normal and worst situations.

Acknowledgments

We would like to thank Greg Hand and Paul McKenna of ITS for providing Telecommunication Analysis Services (The Institute for Telecommunication Sciences (ITS), created in 1967 out of the engineering area of the Central radio Propagation Laboratory of National Bureau of Standards (CRPL/NBS) is now a part of the National Telecommunications and Information Administration (NTIA) of the U.S. Department of

Commerce). We are also grateful to Dan Bathker for his help in calculating transmitter antenna near-field gain. This paper is reviewed by Dr. Anil Kantak.

References

- [1] International mobile telecommunications-2000 (IMT-2000), Rec. ITU-R M.687, 1997.
- [2] Framework for services supported on International mobile telecommunications-2000 (IMT-2000), Rec. ITU-R M.816, 1997.
- [3] Guidelines for evaluation of radio transmission technologies for IMT-2000, Rec. ITU-R M.1225, 1997.
- [4] ITU finds way forward for 3G mobile systems, pp18, ITU News, 4/99, 1999.
- [5] Spectrum considerations for implementation of international mobile telecommunications-2000 (IMT-2000) in the band 1885-2025 MHz and 2110-2200 MHz, Rec. ITU-R M.1036, 1999.
- [6] European Radiocommunications Committee Decision on the harmonised utilisation of spectrum for terrestrial Universal Mobile Telecommunications System (UMTS) operating within the bands 1900-1980 MHz, 2010-2025 MHz and 2110-2170 MHz, (ERC/DEC/(99)HH), ERC 25th meeting, Helsinki 10-12 March 1999.
- [7] Ojanpera, T., et al., An overview of third-generation wireless personal communications: A European perspective, pp59, IEEE Personal Communications, December 1998.
- [8] Dahlman, E., et al., UMTS/IMT-2000 based on wideband CDMA, pp70, IEEE Communications Magazine, September 1998.
- [9] Prediction procedure for the evaluation of microwave interference between stations on the surface of the earth at frequencies above about 0.7 GHz, Recommendation ITU-R P.452-9, 1999.
- [10] Determination of the coordination area of an earth station operating with a geostationary space station and using the same frequency band as a system in a terrestrial service, Recommendation ITU-R IS.847-1, 1993.
- [11] Propagation data required for the evaluation of coordination distances in the frequency range 100 MHz to 105 GHz, Recommendation ITU-R P.620-4, 1999.
- [12] Christian Ho, Miles Sue, Ted Peng, Peter Kinman and Harry Tan, Interference Effects of Deep Space Network Transmitters on IMT-2000/UMTS Receivers at S-band, *JPL TMO Progress Report*, 42-142, August 15, 2000.
- [13] Propagation by diffraction, Recommendation ITU-R P.526-6, 1999.
- [14] Attenuation by Atmospheric Gases, Recommendation ITU-R P.676-4, 1999.
- [15] Radio Regulations, Appendix S7, Method for the determination of the coordination area around an earth station in frequency bands between 1 GHz and 40 GHz shared between space and terrestrial radiocommunication services (Former Appendix 28), Edition, 1990, Revised, 1997.
- [16] Mathematical model of average and related radiation patterns for line-of-sight point-to-point radio-relay system antennas for use in certain coordination studies and interference assessment in the frequency range from 1 GHz and to about 70 GHz, Recommendation ITU-R F.1245-1, 2000.
- [17] Ramsay, J.F., Tubular beams from radiating apertures, *Advances in Microwaves*, Vol. 3, Edited by L. Young, Academic Press, 1968.
- [18] Jamnejad, V., DSN Radio frequency interference pattern modeling, JPL Interoffice Memo, Feb. 4, 1999.
- [19] Rice, P.L., et al., Transmission loss predictions for tropospheric communication circuits, Vol. I, National Bureau of Standards, US Department of Commerce, Washington, DC, Technical Note 101, January, 1, 1967.
- [20] Rice, P.L., et al., Transmission loss predictions for tropospheric communication circuits, Vol. II, National Bureau of Standards, US Department of Commerce, Washington, DC, Technical Note 101, January, 1, 1967.
- [21] Medidas De Cobertura Radioelectrica, Antenna DSS-63, MDSCC, Ministerio De Fomento, Secretaria General De Comunicaciones, Noviembre, 1999.